Efficient Numerical Methods for Simulation of High-Frequency Active Devices

Masoud Movahhedi, *Student Member, IEEE*, and Abdolali Abdipour, *Member, IEEE*

***Abstract*—We present two new numerical approaches for physical modeling of high-frequency semiconductor devices using filter-bank transforms and the alternating-direction implicit finite-difference time-domain method. In the first proposed approach, a preconditioner based on the filter-bank and wavelet transforms is used to facilitate the iterative solution of Poisson's equation and the other semiconductor equations discretized using implicit schemes. The second approach solves Maxwell's equations which, in conjunction with the semiconductor equations, describe the complete behavior of high-frequency active devices, with larger time-step size. These approaches lead to the significant reduction of the full-wave simulation time. For the first time, we can reach over 95% reduction in the simulation time by using these two techniques while maintaining the same degree of accuracy achieved using the conventional approach.**

***Index Terms*—Alternating-direction implicit finite-difference time-domain (ADI-FDTD) method, filter-bank transforms, full-wave analysis, global modeling, high-frequency devices, preconditioning.**

I. Introduction

MODERN high-frequency electronics are based on technologies such as monolithic microwave integrated circuits (MMICs) with a large number of closely packed passive and active structures, several levels of transmission lines, and discontinuities operating at high speeds and frequencies and sometimes over very broad bandwidths. It is thus anticipated that the design of MMICs should involve robust design tools that would simulate all of the circuit elements simultaneously. The possibility of achieving this type of modeling is addressed by full-wave device analysis and global circuit modeling presented in [1]–[5].

The main issue in the global modeling all elements of the high-frequency circuits is the full-wave analysis of their active devices, which has been considered in this study. In the full-wave analysis, the equations that describe the transport physics in conjunction with Maxwell's equations must be solved to predict the interactions between the carriers and the propagating wave inside the devices [1], [2]. We must note that some phenomena such as imperfection in the crystal structure of the semiconductor cannot be exactly considered in the equations. Imperfections that perturb the periodicity of the crystal [6] can contribute significantly to the overall device behavior and are still very difficult to model.

Manuscript received October 10, 2005; revised January 20, 2006. This work was supported in part by the Iran Telecommunication Research Center.

The authors are with the Department of Electrical Engineering, AmirKabir University of Technology (Tehran Polytechnic), Tehran, Iran (e-mail: movahhedi@aut.ac.ir; abdipour@aut.ac.ir).

Digital Object Identifier 10.1109/TMTT.2006.872937

The full-wave analysis involves a fair amount of advanced numerical techniques and different algorithms that results in a very expensive computational cost [5]. Therefore, there is an imperative need to present a new approach to reduce the simulation time, while maintaining the same degree of accuracy presented by the global modeling techniques. Due to the high complexity of the equations, usually the finite-difference time-domain (FDTD) technique is used to solve them. In this numerical technique, a possible approach for reducing the simulation time is to use multiresolution nonuniform grids that can be implemented using interpolating wavelets [7], [8]. Wavelets were applied to the drift-diffusion model [7]. A new approach has been developed for applying wavelets to the full hydrodynamic model [8]. The interpolating wavelets can adaptively refine the mesh in domains where the unknowns quantities vary rapidly. This also leads to considerable reduction in the number of unknowns and the simulation time. The best situation shows about a 75% reduction in CPU time [8].

In this paper, we propose to use two approaches for reducing the simulation time of the full-wave analysis. The first approach improves the simulation time and facilitates the steady-state dc solutions which are used as the initialization values in the full-wave analysis. The second one accelerates the transient simulation to obtain the time-domain ac solutions of the modeling.

In the conventional approach for full-wave analysis using the FDTD method, all of the equations that include the time derivative (e.g., hydrodynamic and Maxwell's equations) are represented by explicit FD schemes [1]. However, solving Poisson's equation (as an elliptic equation) leads to a large system of linear equations, $Ax = b$. Therefore, one of the key factors for simulation time reduction of active microwave devices is to decrease the solution time of the equation system, $Ax = b$. Here, a new filter-bank-based preconditioning method [9] is used to facilitate the iterative solution of Poisson's equation.

Another proposed approach accelerates the time-domain ac solution. Recently, a new method, called the alternating-direction implicit FDTD (ADI-FDTD) method, to solve Maxwell's curl equations has been introduced [10], [11]. This method is an attractive alternative to the standard FDTD due to its unconditional stability with moderate computational overhead. The unconditional stability means that the ADI-FDTD method is free of the Courant–Friedrich–Levy (CFL) stability restraint, allowing any choice of Δt for a stable solution. The ADI-FDTD can be particularly useful for problems involving devices with fine geometric features that are much smaller than the wavelengths of interest. Here, the unconditionally stable FDTD method has been proposed for solving Maxwell's equations, which together with the semiconductor equations perform the full-wave modeling. This allows using a larger

time-step size that leads significantly to CPU time reduction while maintaining the same degree of accuracy achieved using the conventional approach.

This paper is organized as follows. Section II gives a brief review of the full-wave analysis. Section III presents the conventional numerical schemes which are used in the simulation and are based on the FDTD method. A filter-bank based preconditioner as one of the proposed approaches along with its application to a device are provided in Section IV. Section V describes the ADI-FDTD method as another approach and presents its results. Finally, conclusions are drawn in Section VI.

II. Full-Wave Analysis

Usually in the submillimeter and upper millimeter wave range, the active device dimensions become comparable to the wavelength. Therefore, it cannot be treated as a point or a lumped element any more. The high-frequency aspects, including distributed effects, propagation delays, electron transmit time, parasitic elements, and discontinuity effects become important and have to be thoroughly investigated. The most accurate approaches for modeling of these high-frequency active devices are the full-wave analysis techniques. The full-wave time-domain simulation couples a three-dimensional (3-D) time-domain solution of Maxwell's equations (EMS model) with the active device model (AD model) [1].

A. AD Model

The AD model used for simulation is a 3-D large-signal EM physical model. It is based on the moments of the Boltzmann's transport equation that is obtained by integration on the momentum space. The integration results in a strongly coupled, highly nonlinear set of partial differential equations called the conservation equations [12]. These equations provide a time-dependent self-consistent solution for the carrier density, energy, and momentum, which are given as follows.

- *Current continuity*

$$\frac{\partial n}{\partial t} + \nabla \cdot (n\vec{v}) = 0. \tag{1}$$

- *Energy conservation*

$$\frac{\partial (n\omega)}{\partial t} + \nabla \cdot (n\vec{v}(\omega + k_B T)) = -qn\vec{v} \cdot (\vec{E} + (\vec{v} \times \vec{B})) - \frac{n(\omega - \omega_0)}{\tau_\omega(\omega)}. \tag{2}$$

- *X-momentum conservation*

$$\frac{\partial (np_x)}{\partial t} + \nabla \cdot (np_x\vec{v}) + \frac{\partial (nk_B T)}{\partial x} = -qn(E_x + (\vec{v} \times \vec{B})_x) - \frac{np_x}{\tau_m(\omega)}. \tag{3}$$

The similar equations are written and used for simulation for momentum in the other directions. In the above equations, n is the electron concentration, $\vec{v}$ is the electron velocity, $\vec{E}$ is the electric field, ω is the electron energy, ω_0 is the equilibrium thermal energy, p is the electron momentum, and k_B is the Boltzmann constant. The energy and momentum relaxation times are given by τ_ω and τ_m, respectively. In steady-state dc analysis and in the source plane, the three conservation equations are solved in conjunction with the Poisson's equation

$$\nabla^2 \varphi = -\frac{q}{\epsilon}(N_d - n) \tag{4}$$

where φ is the electrostatic potential, q is the electron charge, ϵ is the dielectric constant, N_d is the doping concentration, and n is the carrier concentration at any given time. The electric current density distribution $\vec{J}$ inside the active device at any time t is given by

$$\vec{J}(t) = -qn(t)\vec{v}(t). \tag{5}$$

B. EMS Model

The electromagnetic (EM) wave propagation can be completely characterized by solving Maxwell's equations. These equations are first-order linear coupled differential equations relating the field vectors, current densities, and charge densities at any point in space at any time. Maxwell's curl equations are given by

$$\nabla \times \vec{E} = -\frac{\partial \vec{B}}{\partial t} \tag{6}$$

$$\nabla \times \vec{H} = \frac{\partial \vec{D}}{\partial t} + \vec{J} \tag{7}$$

where $\vec{E}$ is the electric field, $\vec{H}$ is the magnetic field, $\vec{D}$ is the electric flux density, and $\vec{B}$ is the magnetic flux density. The fields in Maxwell's equations are updated using the current density estimated by (5).

C. Coupling the Two Models

The coupling between the two models is established by properly transforming the physical parameters (e.g., fields and current densities) from one model to the other. In each time step, the Maxwell's and semiconductor equations should be solved sequentially. First, the Maxwell's equations are solved for the electric and magnetic field distributions using the current density obtained in the previous time step. Then, the obtained EM fields are used in the semiconductor equations to find the new current density. This process is repeated for each time interval [1]. The full-wave analysis procedure includes the following.

1) Steady-State DC Solution (Initialization): The steady-state dc solution for electric fields, current densities, and the other transport parameters are obtained from the semiconductor model by solving Poisson's and hydrodynamic transport equations. These dc solutions serve as the corresponding initial values inside the AD for the coupled model.

2) Time-Domain AC Solution: After completing the initializations, the ac excitation is applied. The time-domain distribution of the EM fields is obtained using Maxwell's equations. These EM fields are used by the semiconductor model to update the current density. More details about ac and dc solutions can be found in [1].

III. Implementation Using the FDTD Method

Because the carrier transport processes are highly nonlinear, the full-wave analysis problem is solved in the time domain. Due to the complexity of the equations and simplicity of the FD schemes formulation [1], usually the FDTD technique is used to solve them. In numerical implementation of the full-wave analysis using FDTD, both the time and space domains must be discretized.

A. Solution of the AD Model

Equations (1)–(3) are coupled, highly nonlinear partial differential equations (PDEs). To decouple these equations in time, an FD-based scheme is used [13]. The mesh for the device simulator has the vector quantities positioned at the midpoint of the cell and the scalar quantities at the nodal points [1]. This mesh implements a spatial leapfrog technique for enhanced stability and reduced numerical dispersion.

In the conventional methods used for full-wave analysis, all of the equations are represented by explicit FD schemes. Since the time-step is determined according to the EM wave stability condition (Maxwell's equations), no gain is achieved by using other FD formulations (e.g., implicit or semi-implicit). Achieving a stable explicit method for the balance equations is challenging. Successful design of the global simulator depends on the development of a computationally efficient method for solving the systems. A simple FD scheme, forward-time central-space (FTCS), consists of a forward Euler scheme in time and central differencing in space [14]. The method is simple to implement and has relatively low computational requirements when compared with more complicated discretization techniques. However, it suffers from instability for this application. The numerical error is caused by the carrier concentration equation. The equation is hyperbolic and convection-dominated in nature. The FTCS method can be applied sufficiently for the energy and momentum equations (2) and (3). The stability of the model can be improved by employing the Upwind and Lax–Wendroff discretization methods for the current continuity equation [14]. The Upwind scheme has the benefit of having low computational requirements with slightly increased difficulty in implementation while increasing stability. The main drawback of using the Upwind scheme is its asymmetric nature, which causes numerical dispersion of unacceptable levels for characterization of high-frequency circuits. The Lax–Wendroff scheme provides for an increase in accuracy, $O(\Delta t)^2 + O(\Delta x)^2$. The Lax–Wendroff scheme provides for additional stability by introducing an equivalent diffusion term; compromising computational and memory efficiency for numerical stability and accuracy of the solution.

It is clear, in numerical implementation using FDTD both time and space domains must be discretized. For accuracy and stability of the FDTD methods, the time- and space-step sizes must always be chosen to be less than the critical values. In the conservation equations system (AD model), the Debye length limits the spatial step to maintain acceptable numerical accuracy and is usually less than the one-tenth the Debye length [14]. The debye Length of the semiconductor can be calculated using the following equation:

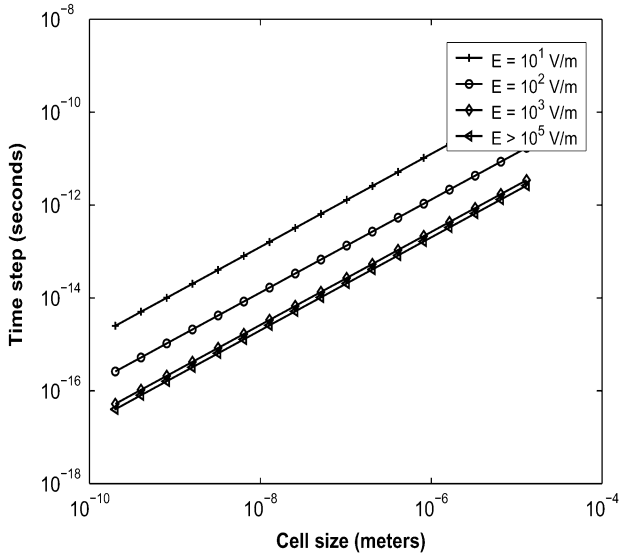

Fig. 1. Time-step size of the AD model versus the E-field and cell size.

$$L_D = \sqrt{\frac{\epsilon_r \epsilon_0 k_B T}{q^2 N_d}} \tag{8}$$

which is a function of the doping level N_d and the other material characteristics ϵ_r [14]. The time-step size in the explicit methods for the semiconductor equations is a function of the average carrier velocity v_d and the spatial step to comply with the following CFL condition for stability and minimizing numerical dispersion [14]:

$$v_d \Delta t \leq \left[\frac{1}{\Delta x^2} + \frac{1}{\Delta y^2}\right]^{-1/2}. \tag{9}$$

The time step is dependent upon the drift velocity and varies inversely to the applied electric field, as seen in Fig. 1. The figure presents a set of parametric curves showing relationship among the electric field and space- and time-steps.

B. Solution of the EMS Model

In all previous works [1], [7], [8], the time-domain solution of Maxwell's equations in the full-wave analysis is obtained using the explicit Yee's method [15]. The spatial increment step of the EMS model is limited by the maximum frequency $f_{\max}$ of the excitation for a basic Yee FDTD model and is usually smaller than one-tenth of the wavelength. In conventional FDTD scheme for solving the EMS model (explicit method), the time-step size must be small enough so that it satisfies the following CFL stability condition:

$$v_{p_{\max}} \Delta t \leq \left[\frac{1}{\Delta x^2} + \frac{1}{\Delta y^2} + \frac{1}{\Delta z^2}\right]^{-1/2} \tag{10}$$

where $v_{p_{\max}}$ is the maximum-wave phase velocity within the model.

IV. Filter-Bank-Based Preconditioner

Solving elliptic PDEs or using implicit methods for solving time-dependent PDEs results in a large system of linear equations, $Ax = b$. The complexity of the problems is often too high for using a direct solver. Therefore, one has to rely on iterative methods [16]. Convergence of such methods is often dependent on the condition numbers of the operator matrices A; small condition numbers guarantee a fast convergence to the solution, whereas large condition numbers often imply that the convergence will be slow. For instance, solving Poisson's equation on a large or nonuniform grid leads to a matrix with a large condition number. In this case, an effective preconditioning of matrix A is usually required in order to keep the number of iterations small [16]. Using genetic-based algorithms described and used in [17] is another approach for solving the problem. In [17], it is shown that a genetic-based algorithm converges independent of the condition number of matrix A obtained from Poisson's equation. Although genetic algorithms are unconditionally stable algorithms, their convergence is very slow. Therefore, these algorithms cannot meet the urgent need of the full-wave analysis of high-frequency semiconductor devices with short simulation time. Here, we propose an efficient method that not only guarantees the solution accuracy, but also increases the speed of convergence.

As mentioned before, the size of matrix A, in the system of $Ax = b$, is very large and has a large condition number. In this case, an iterative technique is usually employed, and an effective preconditioner of matrix A is required in order to obtain fast convergence [16]. Generally, the better conditioned system leads to an accelerated convergence in the iterative solution [18]. Some well-documented preconditioning methods such as the incomplete lower-upper (ILU) factorization and polynomial preconditioning methods [19], [20] can be effective. However, they usually require well above $O(N)$ operations. Recently, an interesting preconditioning method based on the filter-bank and wavelet transforms was proposed [21]. Its main advantage is its low computational cost, which is reduced to $O(N)$. In this section, we will use this new preconditioner to precondition matrix A that resulted from Poisson's equation which must be solved to obtain steady-state solution and in the source plane in transient and ac simulation.

A. Standard Poisson's Equation

The two-dimensional (2-D) Poisson's equation has the following form:

$$\frac{\partial^2 \varphi}{\partial x^2} + \frac{\partial^2 \varphi}{\partial y^2} = f(x, y). \tag{11}$$

Here, we focus on the FD discretization of Poisson's equation. The above equation can be discretized as the following:

$$\frac{\varphi_{i+1,j} - 2\varphi_{i,j} + \varphi_{i-1,j}}{(\Delta x)^2} + \frac{\varphi_{i,j+1} - 2\varphi_{i,j} + \varphi_{i,j-1}}{(\Delta y)^2} = f(x_i, y_j) \tag{12}$$

where the subscripts (i, j) denote the (i, j)th grid point on the x–y plane. Equation (12) can be written in a matrix form $Ax = b$, where the vectors x and b contain the variables $\varphi_{i,j}$ and $f(x_i, y_j)$, respectively, which are lined up in a systematic order.

B. Modified Poisson's Equation

In the conventional numerical methods used in the full-wave analysis, all of the semiconductor equations are represented by explicit FD schemes [1]. It is important to note that, in this study, an unconditionally stable method is used to solve Maxwell's equations. Thus, we can consider implicit methods to solve AD model equations to reach to the larger time-steps. Here, we consider one of the existing implicit schemes for semiconductor equations. In this scheme, Poisson's equation is considered as follows and called the modified Poisson's equation [22].

During solving for the potential φ^{t+1} at time level $(t+1)$, the carrier concentration n^{t+1} at $(t + 1)$ is not available. However, this can be approximated in the following ways [23]:

$$\nabla^2 \varphi^{t+1} = -\frac{q}{\epsilon}(N_d - n^{t+1}). \tag{13}$$

Expanding n^{t+1} using a Taylor series gives

$$n^{t+1} = n^t + \Delta t \left(\frac{\partial n}{\partial t}\right)_t + O(\Delta t^2). \tag{14}$$

Ignoring second-order and higher order terms in time $O(\Delta t^2)$ and substituting for $(\partial n/\partial t)_t$ from the current continuity (1) yields

$$n^{t+1} = n^t + \Delta t \nabla \cdot (-n^t \mu \vec{\nabla} \varphi^{t+1} + \vec{\nabla}(D n^t)) \tag{15}$$

when defining carrier mobility as $\mu \equiv q\tau_p/m^\star$ and diffusion coefficient as $D \equiv \mu k_B T/q$.

Hence, (13) can be rewritten as follows:

$$\nabla^2 \varphi^{t+1} \left(1 + \frac{q\mu\Delta t}{\epsilon} n^t\right) + \frac{q\mu\Delta t}{\epsilon} \vec{\nabla} \varphi^{t+1} . \vec{\nabla} n^t = \frac{q}{\epsilon}(-N_d + n^t + D\Delta t \nabla^2 n^t). \tag{16}$$

The modified Poisson's equation (16) is solved for φ^{t+1} using the full implicit method. The above modification of Poisson's equation allows one to solve Poisson's and carrier continuity equations sequentially. Numerical stability is maintained for Δt as high as $50\Delta t_{\text{explicit}_{\max}}$, where $\Delta t_{\text{explicit}_{\max}}$ is the maximum allowable time-step in the explicit scheme obtained using (9), [23].

C. Construction of the Preconditioner

If we consider a PDE with special boundary conditions and assume that this problem is discretized with a FD method, a system of linear equations can be obtained as $Ax = b$. We want to use the filter-bank transform to precondition the operator. The idea is that the W parts of the transformed operator will be diagonally dominant, whereas the V is not, but this part is very small and can be directly inverted [21]. The filter-bank transform of matrix A is defined as

$$\tilde{A} = TAT^T \tag{17}$$

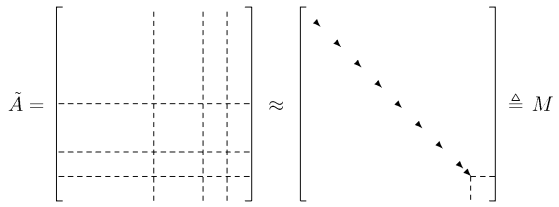

Fig. 2. Structure of the matrix representation of a transformed operator.

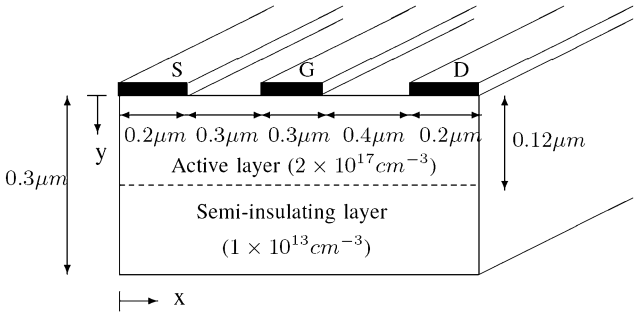

Fig. 3. Structure of a MESFET transistor for full-wave analysis.

where matrix T performs $(n-n_0)$ steps in the filter-bank transform T^{n-n_0}: $V^n \rightarrow (\oplus_{j=1}^{n-n_0} W^{n-j}) \oplus V^{n_0}$ (see [24] for notation and details). In general, the matrix representation of the transformed operator is shown in Fig. 2. Here, M is the approximation of the transformed operator. From its inverse that can be computed very easily, we will construct the preconditioner. Our approximation of $\tilde{A}$ is chosen as in Fig. 2 [24] as follows:

$$M_{i,j} = \begin{cases} \tilde{A}_{i,j}, & i=j, i \in W^k; \quad n_0 \le k < n \\ \tilde{A}_{i,j}, & i,j \in V^{n_0} \\ 0, & \text{otherwise.} \end{cases} \tag{18}$$

Now, the filter bank preconditioning algorithm can be described by the following steps.

Step 1) Take the filter-bank transform to get $\tilde{A} = TAT^T$.

Step 2) Create the approximation of the transformed operator (M) by (18).

Step 3) Use M^{-1} as preconditioner to solve $\tilde{A}\tilde{x} = \tilde{b}$, where $\tilde{b} = Tb$.

Step 4) Apply backward filter-bank transform to $\tilde{x}$ to obtain $x = T^T\tilde{x}$.

According to the problem dimension, different filter-bank transforms can be used, i.e., for n-dimensional problems, we can use the n-dimensional filter-bank transforms that are explained in detail in [21]. In the following, we use the tensor product filter-bank transform, which is called the 2-D transform, for preconditioning. Also, we use Daubechies wavelets for wavelet transforms and δ_1 and δ_3 filter-banks for filter-bank transforms [24].

D. Application to a Device

Fig. 3 shows the GaAs MESFET structure used to demonstrate the potential of the proposed preconditioner. This structure is discretized by a uniform mesh of $65\Delta x \times 32\Delta y$. Dirichlet boundary conditions are used at the electrodes, while Neumann boundary conditions are used at the other walls. The size of matrix A, arising from the standard and modified Poisson's equation, is (2048×2048). First, consider the standard Poisson's equation. The condition number of matrix A in this situation is 4051, and we apply the proposed filter-bank-based and wavelet-based preconditioners to it to reduce this condition number. In Tables I and II, we present the variation of condition number of the preconditioned matrix according to the type of filter-bank and wavelet transforms and to the number of steps in the transform. Transform steps determine the size of nondiagonal part of matrix M called $\acute{M}$. We have used the tensor product (2-D) transforms for preconditioning. Fig. 4 shows the convergence behavior of the proposed preconditioner for different filter-bank and wavelet 2-D transforms. Convergence behavior of the preconditioned system is similar to the variation of its condition number. As can be seen, the convergence rate increases as the filter-bank is of lower order and as the decomposition level decreases. However, for the Daubechies wavelet transforms, the convergence rate increases as the wavelet is of higher order and as the decomposition level increases. We found that preconditioning using the δ_1 filter-bank transform converges faster than the other filter-bank and wavelet transforms. By increasing the number of steps in the transform, the size of the nondiagonal part of M decreases. Therefore, the computational complexity of the preconditioning method, which is equal to $O(N + \acute{M}^3)$, can be reduced by increasing the number of steps in the transform [24]. It is interesting that we can obtain both good conditioning and low computational cost by using δ_1 filter-bank transform. To compare the performance of the used preconditioner (i.e., filter-bank-based preconditioner) with the well-known preconditioning methods, the convergence rate of the ILU preconditioner has been illustrated in Fig. 4. As is clearly seen, in almost all cases, for different filter-bank and wavelet transforms

TABLE I
CONDITION NUMBER OF THE PRECONDITIONED LAPLACIAN OPERATOR MATRIX CORRESPONDING TO THE MESFET STRUCTURE FOR DIFFERENT FILTER-BANK TRANSFORMS

Type of filter-bank	Name	$\acute{M}$	Condition number
δ_1	$Delta1_{22}$	$(2^4.2^3) \times (2^4.2^3)$	592
δ_1	$Delta1_{32}$	$(2^3.2^3) \times (2^3.2^3)$	698
δ_1	$Delta1_{33}$	$(2^3.2^2) \times (2^3.2^2)$	820
δ_1	$Delta1_{43}$	$(2^2.2^2) \times (2^2.2^2)$	984
δ_3	$Delta3_{22}$	$(2^4.2^3) \times (2^4.2^3)$	774
δ_3	$Delta3_{32}$	$(2^3.2^3) \times (2^3.2^3)$	959
δ_3	$Delta3_{33}$	$(2^3.2^2) \times (2^3.2^2)$	1159
δ_3	$Delta3_{43}$	$(2^2.2^2) \times (2^2.2^2)$	1300

TABLE II
CONDITION NUMBER OF THE PRECONDITIONED LAPLACIAN OPERATOR MATRIX CORRESPONDING TO THE MESFET STRUCTURE FOR DIFFERENT WAVELET TRANSFORMS

Type of wavelet	Name	$\acute{M}$	Condition number
D_4	$Dab4_{22}$	$(2^4.2^3) \times (2^4.2^3)$	1140
D_4	$Dab4_{32}$	$(2^3.2^3) \times (2^3.2^3)$	844
D_4	$Dab4_{33}$	$(2^3.2^2) \times (2^3.2^2)$	810
D_4	$Dab4_{43}$	$(2^2.2^2) \times (2^2.2^2)$	790
$D_2(Haar)$	$Dab2_{22}$	$(2^4.2^3) \times (2^4.2^3)$	1940
$D_2(Haar)$	$Dab2_{32}$	$(2^3.2^3) \times (2^3.2^3)$	1412
$D_2(Harr)$	$Dab2_{33}$	$(2^3.2^2) \times (2^3.2^2)$	1381
$D_2(Harr)$	$Dab2_{43}$	$(2^2.2^2) \times (2^2.2^2)$	1250

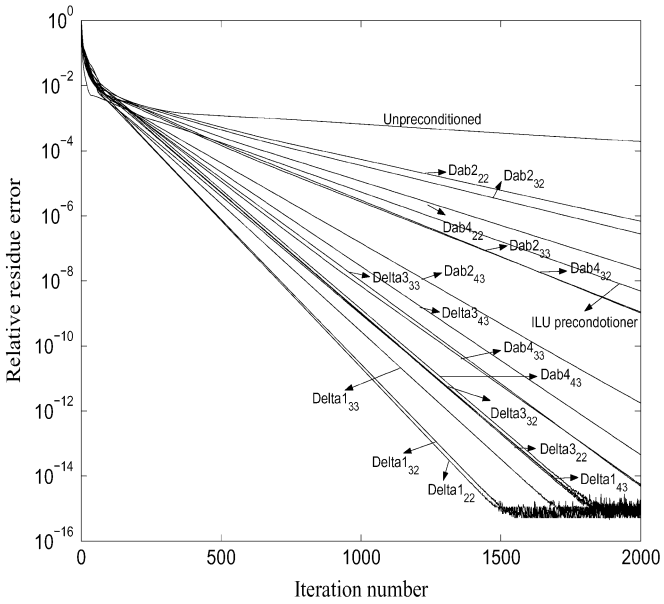

Fig. 4. Convergence behavior of the ILU preconditioner and the proposed preconditioner system on the standard Poisson's equation by different wavelet and filter-bank transforms.

TABLE III
CONDITION NUMBER OF THE PRECONDITIONED MATRIX ARISING FROM MODIFIED POISSON'S EQUATION CORRESPONDING TO THE MESFET STRUCTURE FOR DIFFERENT FILTER-BANK TRANSFORMS

Type of filter bank	Name	$\acute{M}$	Condition no.
δ_1	$Delta1_{22}$	$(2^4.2^3) \times (2^4.2^3)$	2099
δ_1	$Delta1_{32}$	$(2^3.2^3) \times (2^3.2^3)$	2528
δ_1	$Delta1_{33}$	$(2^3.2^2) \times (2^3.2^2)$	2694
δ_1	$Delta1_{43}$	$(2^2.2^2) \times (2^2.2^2)$	3381
δ_3	$Delta3_{22}$	$(2^4.2^3) \times (2^4.2^3)$	2738
δ_3	$Delta3_{32}$	$(2^3.2^3) \times (2^3.2^3)$	3448
δ_3	$Delta3_{33}$	$(2^3.2^2) \times (2^3.2^2)$	3759
δ_3	$Delta3_{43}$	$(2^2.2^2) \times (2^2.2^2)$	4786

TABLE IV
CONDITION NUMBER OF THE PRECONDITIONED MATRIX ARISING FROM MODIFIED POISSON'S EQUATION CORRESPONDING TO THE MESFET STRUCTURE FOR DIFFERENT WAVELET TRANSFORMS

Type of wavelet	Name	$\acute{M}$	Condition number
D_4	$Dab4_{22}$	$(2^4.2^3) \times (2^4.2^3)$	3976
D_4	$Dab4_{32}$	$(2^3.2^3) \times (2^3.2^3)$	3248
D_4	$Dab4_{33}$	$(2^3.2^2) \times (2^3.2^2)$	3246
D_4	$Dab4_{43}$	$(2^2.2^2) \times (2^2.2^2)$	3199
$D_2(Haar)$	$Dab2_{22}$	$(2^4.2^3) \times (2^4.2^3)$	6664
$D_2(Haar)$	$Dab2_{32}$	$(2^3.2^3) \times (2^3.2^3)$	5783
$D_2(Harr)$	$Dab2_{33}$	$(2^3.2^2) \times (2^3.2^2)$	5634
$D_2(Harr)$	$Dab2_{43}$	$(2^2.2^2) \times (2^2.2^2)$	5454

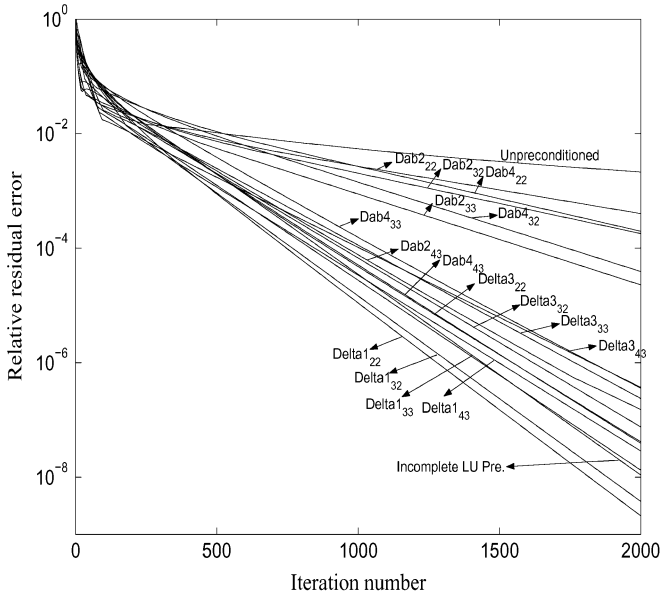

Fig. 5. Convergence behavior of the ILU preconditioner and the proposed preconditioner system on the modified Poisson's equation by different wavelet and filter-bank transforms.

and decomposition levels, the convergence rate is faster than the ILU(0) preconditioner.

We now consider the modified Poisson's equation. Solving (16) for $\varphi_{i,j}^{t+1}$ leads to a system of linear equations, $Ax = b$, where matrix A is a function of Δt and carrier density distribution n^t. This situation is established in implicit discretization of carrier continuity and the other semiconductor equations. It is important to note that, when an explicit scheme is used to solve hydrodynamic model equations, the maximum allowable time step is about $\Delta t_{\text{explicit}} = 0.001$ ps. However, when the equations are discretized with the above implicit scheme, the method will be stable for very large Δt; for instance, $\Delta t = 50\Delta t_{\text{explicit}}$. In this study, the proposed method is applied to matrix A when $t = 0$, i.e., $n = N_d$ and $\Delta t = 0.01$ ps. The condition number of this matrix is 11 607, and we apply the proposed filter-bank-based preconditioner to A. In Tables III and IV, we present the variation of condition number of the preconditioned matrix according to the type of filter-bank and wavelet transforms and to the decomposition levels. Fig. 5 shows the convergence behavior of the proposed preconditioner for different filter-bank and wavelet 2-D transforms. It is observed that the convergence behavior is similar to the standard Poisson's equation. Although the performance of the used preconditioner is better when applied to the Laplacian operator matrix in standard Poisson's equation, for the δ_1 filter-bank transform with different decomposition levels, the convergence rate is faster than that for the ILU(0) preconditioner.

As the results show, the convergence rate of the preconditioning scheme used, especially by δ_1 filter-bank transform, is faster than the well-known ILU method. Moreover, the computational cost of the considered method is as low as $O(N)$, which is better than any other methods. Here, we only investigated performance of the preconditioner on Poisson's equation (i.e., standard and modified equations). However, it seems that the proposed method can work very well on the other matrices coming from the conservation equations that are discretized using implicit schemes.

V. UNCONDITIONALLY STABLE FDTD METHOD

In Section III, the conventional implementation of the full-wave analysis using the FDTD method was described. It was mentioned that, in the full-wave simulation, the AD model and the EMS model must be solved simultaneously. Therefore, in its implementation using the FD method, the cell and time-

step sizes must be sufficiently small in order to satisfy the accuracy and stability conditions of both models. In almost all cases of the full-wave analysis, the conservation transport equations impose cell size. This is because of the smaller Debye length of the semiconductor compared with the signal wavelength. In addition, Maxwell's equations solved by the conventional FDTD method will force the time-step size. This results from a larger phase velocity of the wave compared with the carrier drift velocity.

To the best of our knowledge, in all previous works done to reduce the simulation time of the full-wave analysis and global modeling, these discretization parameters have been taken as fixed. In these works, the proposed techniques to decrease simulation time, such as using nonuniform mesh generated by wavelet, show only about 75% reduction in CPU run time [8]. In this paper, we significantly reduce the simulation time by increasing the time-step size of the FDTD technique. We propose to use the ADI-FDTD method, which allows any choice of Δt for a stable scheme, to solve the EMS model in the full-wave analysis. Thus, only the CFL stability condition of the AD model limits the chosen time-step size. Consequent, the CPU run time will be reduced significantly.

A. ADI-FDTD Method

The standard FDTD scheme is a well-established technique for simulating EM systems. Two major limitations of the FDTD method are the simulation errors and execution time. The simulation errors are due to discretizing the space and time and are measured typically through the amount of numerical dispersion. Long execution times result from the requirement of a time-domain signal to ring out or reach steady state. The execution time of an FDTD simulation is inversely proportional to the size of the chosen time-step. A major limitation of existing FDTD schemes is the conditionally stable nature of the technique, since the CFL condition must be satisfied when this method is used. Recently, a new algorithm introduced by Namiki [10] and Zheng *et al.* [11] has been proposed in order to eliminate the constraints of the CFL condition. This new algorithm is based on the ADI method and is applied to the Yee's staggered cell to solve Maxwell's equation. The ADI method is known as the implicit-type FD algorithm, which has the advantage of ensuring a more efficient formulation and calculation than other implicit methods in the case of multidimensional problems.

For explanation of the ADI-FDTD formulation, we consider the following equation from system (6):

$$\frac{\partial H_x}{\partial t} = \frac{1}{\mu}\left(\frac{\partial E_y}{\partial z} - \frac{\partial E_z}{\partial y}\right). \tag{19}$$

By applying the ADI principle, the computation of (19) for the FDTD solution marching from the nth time-step to the $(n+1)$th time-step is broken up into two computational subadvancements: the advancement from the nth time-step to the $(n+1/2)$th time-step and the advancement from the $(n+1/2)$th time-step to the $(n+1)$th time-step. More specifically, the two substeps are as follows.

Step 1) For the first half-step, i.e., at the $(n+1/2)$th time step, the first partial derivative on the right-hand side (rhs) of (19), $\partial E_y/\partial z$, is replaced with an implicit difference approximation of its unknown pivotal values at the $(n+1/2)$th time step, while the second partial derivatives on the rhs, $\partial E_z/\partial y$, is replaced with an explicit FD approximation in its known values at the previous nth time step. In other words,

$$\mu_{i,j+\frac{1}{2},k+\frac{1}{2}}\left(\frac{H_x|^{n+\frac{1}{2}}_{i,j+\frac{1}{2},k+\frac{1}{2}} - H_x|^{n}_{i,j+\frac{1}{2},k+\frac{1}{2}}}{\Delta t/2}\right) = \frac{E_y|^{n+\frac{1}{2}}_{i,j+\frac{1}{2},k+1} - E_y|^{n+\frac{1}{2}}_{i,j+\frac{1}{2},k}}{\Delta z} - \frac{E_z|^{n}_{i,j+1,k+\frac{1}{2}} - E_z|^{n}_{i,j,k+\frac{1}{2}}}{\Delta y}. \tag{20}$$

Step 2) For the second half time-step (i.e., at $(n+1)$th time step), the second term on the rhs, $\partial E_z/\partial y$, is replaced with an implicit FD approximation of its unknown pivotal values at the $(n+1)$th time step, while the first term $\partial E_y/\partial z$ is replaced with an explicit FD approximation in its known values at the previous $(n+1/2)$th time-step. In other words,

$$\mu_{i,j+\frac{1}{2},k+\frac{1}{2}}\left(\frac{H_x|^{n+1}_{i,j+\frac{1}{2},k+\frac{1}{2}} - H_x|^{n+\frac{1}{2}}_{i,j+\frac{1}{2},k+\frac{1}{2}}}{\Delta t/2}\right) = \frac{E_y|^{n+\frac{1}{2}}_{i,j+\frac{1}{2},k+1} - E_y|^{n+\frac{1}{2}}_{i,j+\frac{1}{2},k}}{\Delta z} - \frac{E_z|^{n+1}_{i,j+1,k+\frac{1}{2}} - E_z|^{n+1}_{i,j,k+\frac{1}{2}}}{\Delta y}. \tag{21}$$

Applying the same procedure to all the other five scalar differential equations of Maxwell's equations, one can obtain the complete set of the implicit unconditionally stable FDTD formulas [11]. Using the above method to solve Maxwell's equations creates an unconditionally stable 3-D FDTD method.

B. Simulation Results

In order to demonstrate the performance of the proposed approach, first the GaAs MESFET transistor shown in Fig. 3 is considered. This transistor has an EMS excitation with $f_{\max} = 100$ GHz, large applied electric field, and heavily doped $N_d = 2\times10^{17}$ cm^{-3}. The cell size of the EMS model is approximately 10^{-4} m, and the AD model cell size is approximately 10^{-8} m, according to (8). Because two equation systems must be solved simultaneously, the cell size is chosen equal to 0.01 μm [1]. For the given cell size, the EMS and AD time-step sizes are about 10^{-17} and 10^{-15} s, respectively, as presented in (10) and Fig. 1. For full-wave simulation, the smallest time-step size is chosen, i.e., $\Delta t = 0.01$ fs. [1].

In the above example, by using the ADI-FDTD method to solve the EMS model, the time-step Δt can be increased from 10^{-17} to 10^{-15} s. This means that the number of necessary time-steps for simulation will be reduced by a factor of 100. This must be mentioned because the ADI-FDTD method is an implicit technique, so its computational cost and calculation time

in each time-step are more than for the conventional FDTD method, which is an explicit time-marching technique. In our case (i.e., MESFET transistor), simulations show that the calculation time of the ADI-FDTD in each time step is about five times the calculation time of the conventional FDTD. Therefore, the full-wave simulation by the ADI-FDTD method will be done 20 times faster than the conventional FDTD method. In other words, this method shows about 95% reduction in CPU run time.

To simulate the infinite space surrounding the structure, in the implementation of the ADI-FDTD method, absorbing boundaries must be used. The choice of absorbing boundaries is very critical to the overall stability of the FD scheme. It has been observed that, for a long time simulation, instability is likely to occur if the absorbing boundary conditions are not chosen correctly. It must be noted that the unconditional property of the ADI-FDTD method can be violated if the boundary condition equations are not discretized properly. It was found that, in our simulation, where the CFL number is very large (about 100) and the cell size in direction z is larger than in the other directions (i.e., Δz is on the order of micrometers), only using the PML technique for boundary condition causes the ADI-FDTD method to remain unconditionally stable. We have used the split-field PML, which is based on Berenger's original formulation and employed within the ADI-FDTD formulation [25], and its modification [26].

1) Numerical Dispersion Analysis: Although the ADI-FDTD method is unconditionally stable, it has been shown that the accuracy of the numerical results obtained with the method gets worse when time-step increases [27], [28]. This is due to the fact that the numerical dispersion error of the method gets bigger when the time-step increases.

Here, the effect of the large time-steps on the numerical dispersion and the accuracy of the ADI-FDTD method is investigated. In this study, we have used the analytical formula which was presented in [27]. According to this formula, the numerical dispersion of the unconditionally stable ADI-FDTD method is a function of the time-step size and mesh resolution (wavelength per cell size). Dispersion error is defined as $(1 - v_p/c)$, where v_p/c is the normalized numerical phase velocity [27]. The maximum dispersion errors of the ADI-FDTD method for the above example versus the ADI-FDTD time-step size, i.e., CFL number $(=\Delta t_{\mathrm{ADI-FDTD}}/\Delta t_{\mathrm{FDTD}})$, and the frequency are shown in Fig. 6. As can be seen in the figure, for our problem that $\mathrm{CFL} = 100$, $f = 100$ GHz, and the mesh resolution is 10^5, the maximum dispersion error is about $10^{-4}\%$. As mentioned before, in the full-wave simulation, the cell size is imposed by the Debye length, which is much smaller than the practical wavelengths. Thus, the numerical dispersion error of the proposed ADI-FDTD method will be very small, even for very high-frequency simulations (such as 1000 GHz).

2) AC Simulation Result: Finally, for this example, the full-wave simulation results obtained by the proposed approach is investigated. An ac excitation is applied to the gate electrode, which is given as: $V_{\mathrm{gs}}(t) = V_{\mathrm{gs0}} + \Delta v_{\mathrm{gs}} \sin(\omega t)$, where V_{gs0} is the dc bias applied to the gate electrode, ω is the frequency of the applied signal in radians per second, and Δv_{gs} is the peak value of the ac signal (0.1 V). The output drain voltage is estimated

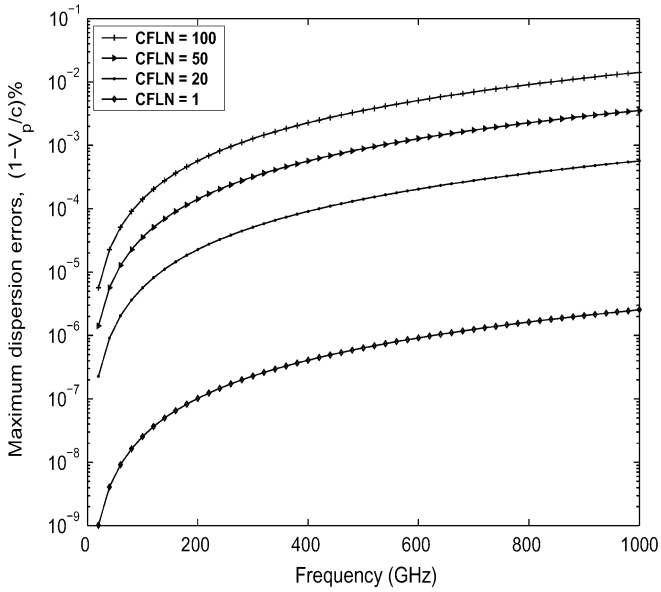

Fig. 6. Maximum dispersion error of the ADI-FDTD method as a function of the CFL and frequency.

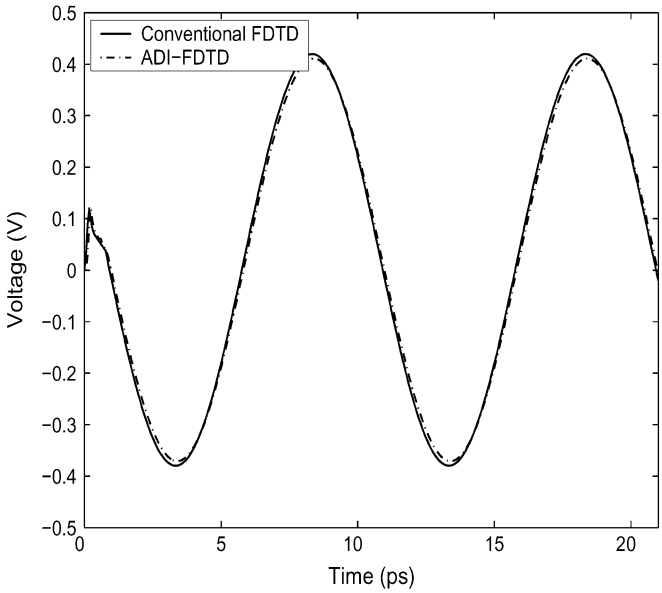

Fig. 7. Output voltage obtained using the conventional FDTD ($\Delta t_{\mathrm{FDTD}} = 10^{-17}$ s) and the ADI-FDTD ($\Delta t_{\mathrm{ADI-FDTD}} = 10^{-15}$ s) methods.

by multiplying the total current by the resistance that defines the dc operating point (Q point) of the transistor [8]. Fig. 7 shows the output voltages obtained using the ADI-FDTD method and the conventional approach. As can be seen, the results in the ADI-FDTD case and the conventional FDTD case are in good agreement.

C. Two-Finger MESFET Transistor

Here, a two-finger MESFET transistor is considered as the second example. Fig. 8 shows a 3-D view of the two-finger simulated transistor. The structure parameters of the transistor used in the simulation are given in Table V. The simulated device is biased to $V_{\mathrm{ds}} = 3$ V and $V_{\mathrm{gs}} = -0.2$ V. The gate length for the transistor is set to 0.25 μm. The dc distribution is obtained

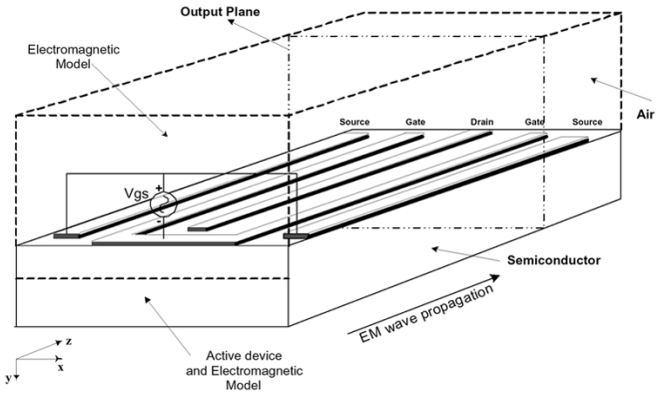

Fig. 8. Generic 3-D view of the simulated two-finger MESFET transistor.

TABLE V
TWO-FINGER MESFET TRANSISTOR PARAMETERS USED IN THE SIMULATION

Drain and Source contact lengths	$0.5\ \mu m$
Gate-Source separation	$0.5\ \mu m$
Gate-Drain separation	$0.45\ \mu m$
Device thickness	$0.4\ \mu m$
Gate length	$0.25\ \mu m$
Active layer thickness	$0.12\ \mu m$
Active layer doping	$2 \times 10^{17}\ cm^{-3}$
DC Gate-Source voltage	$-0.2\ V$
DC Drain-Source voltage	$3\ V$
Operating frequency	$100\ GHz$

by solving the AD model with Poisson's equation. A sinusoidal signal is employed in the ac simulations with a peak value of 100 mV and a frequency of 100 GHz. This signal is applied between the gate and the source electrodes. The excitation is considered to be a plane source at $z = 0$, as shown in Fig. 8. The space and time discretization parameters are chosen similar to those for the previous example, and the proposed methods are used for full-wave analysis of the transistor. The full-wave model is solved for a few RF cycles, i.e., several tens of picoseconds, to avoid the effects of the transients on the ac simulation. Fig. 9 shows the temporal evolution of the output voltage at different sections along the z-direction. The output voltage means the voltage signal between the drain and the source electrodes obtained by the integration on the output plane. Output voltages are shown at device widths of 70, 150, and 210 μm away from the excitation plane. Considering this figure, one should observe the variations of the output voltage with distance along the device width. For short distances, the output voltage amplitude increases along the device width. This phenomena continues until an optimum device width. Beyond this width, the voltage gain decreases. The reasons are due to the nonlinear energy build-up along the device width and due to the phase-velocity mismatch between the EM waves at the gate and drain electrodes. Fig. 9 demonstrates the importance of coupling the EM waves with the semiconductor transport physics for accurate modeling of millimeter-wave transistors.

For comparison purposes, both the ADI-FDTD and the conventional FDTD methods were used for the full-wave analysis of this transistor. Similar to the previous example, the time-step $\Delta t_{\mathrm{FDTD}} = 10^{-17}$ s was chosen with the conventional FDTD method, while $\Delta t_{\mathrm{ADI-FDTD}} = 10^{-15}$ s was chosen with the

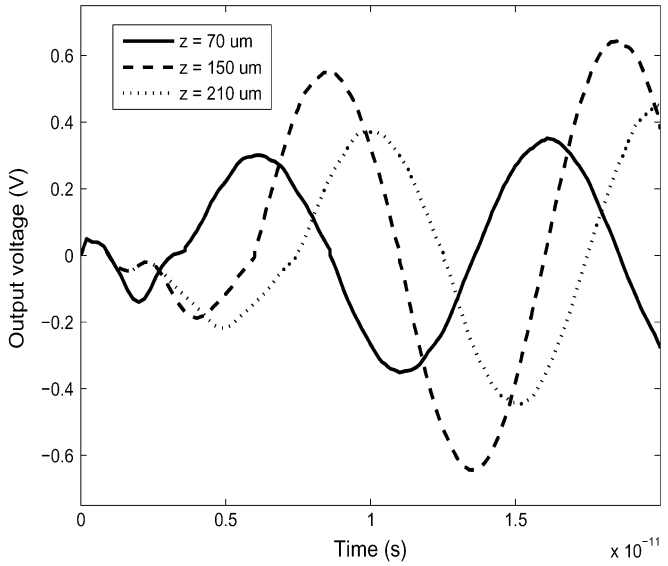

Fig. 9. Output voltage of two-finger transistor when EM-wave propagation and electron–wave interaction (full-wave analysis) are considered at different points in the z-direction.

ADI-FDTD method. With such time-step selections, we found, by trial and error, that the two methods presented similar accuracy. With the FDTD method, 2×10^6 iterations were needed, and 2×10^4 iterations were needed with the ADI-FDTD method. On a Pentium-IV 2.50-GHz PC, it took 1.02 s to finish the simulation of each time-step with the conventional FDTD method and 4.91 s with the ADI-FDTD method. We then concluded preliminarily that a savings factor with the ADI-FDTD method in CPU time is about 20.74 when the conventional FDTD is used as a reference.

VI. CONCLUSION

In this paper, the potentials of the filter-bank transforms and the ADI-FDTD method have been investigated to reduce the simulation time, which is a complicated problem in the full-wave analysis of active microwave devices. Using a new filter-bank-based preconditioner has been suggested for accelerating the iterative solution of a system of linear equations. In the full-wave analysis, this system arise from Poisson's equation and the other semiconductor equations discretized using implicit schemes. This approach accelerates the steady-state dc solutions which are used as the initialization values. The convergence rate of the used preconditioning scheme, by different filter-bank and wavelet transforms (in more cases), is faster than the well-known ILU method. Moreover, the computational cost of the considered method is as low as $O(N)$, which is better than any other methods.

In the time-domain ac analysis of the full-wave simulation, the simulation time is reduced by using larger time-steps. Using the ADI-FDTD method to solve Maxwell's equation allows for increasing the time-step. The proposed approach shows about 95% reduction in the simulation time with a maximum numerical dispersion error of $10^{-4}\%$. Since the size of the local minimum cell in the computational domain (which is imposed by the Debye length) is much smaller than the wavelength, the

error limitation is much larger than the CFL limitation. Therefore, the ADI-FDTD method is more efficient than the conventional FDTD method for full-wave simulation of active microwave/millimeter-wave devices.

ACKNOWLEDGMENT

The authors would like to express their appreciation to Prof. S. Selberherr, Institut für Mikroelektronik, Technische Universität Wien, Vienna, Austria, for his help and guidance.

REFERENCES

[1] M. A. Alsunaidi, S. M. S. Imtiaz, and S. M. El-Ghazaly, "Electromagnetic wave effects on microwave transistors using a full-wave time-domain model," *IEEE Trans. Microw. Theory Tech.*, vol. 44, no. 6, pp. 799–808, Jun. 1996.

[2] S. M. S. Imtiaz and S. M. El-Ghazaly, "Global modeling of millimeter-wave circuits: Electromagnetic simulation of amplifiers," *IEEE Trans. Microw. Theory Tech.*, vol. 45, no. 12, pp. 2208–2216, Dec. 1997.

[3] A. Witzig, C. Schuster, P. Regeli, and W. Fichtner, "Global modeling of microwave applications by combining the FDTD method and a general semiconductor device and circuit simulator," *IEEE Trans. Microw. Theory Tech.*, vol. 47, no. 6, pp. 919–928, Jun. 1999.

[4] P. Ciampolini, L. Roselli, G. Stopponi, and R. Sorrentino, "Global modeling strategies for the analysis of high-frequency integrated circuits," *IEEE Trans. Microw. Theory Tech.*, vol. 47, no. 6, pp. 950–955, Jun. 1999.

[5] R. O. Grondin, S. M. El-Ghazaly, and S. Goodnick, "A review of global modeling of charge transport in semiconductors and full-wave electromagnetics," *IEEE Trans. Microw. Theory Tech.*, vol. 47, no. 6, pp. 817–829, Jun. 1999.

[6] C. T. Sah, "Bulk and inmperfections in semiconductors," *Solid-State Electron,*, vol. 19, pp. 975–990, 1976.

[7] S. Goasguen, M. M. Tomeh, and S. M. El-Ghazaly, "Electromagnetic and semiconductor device simulation using interpolating wavelets," *IEEE Trans. Microw. Theory Tech.*, vol. 49, no. 12, pp. 817–829, Dec. 2001.

[8] Y. A. Hussein and S. M. El-Ghazaly, "Extending multiresolution time-domain (MRTD) technique to the simulation of high-frequency active devices," *IEEE Trans. Microw. Theory Tech.*, vol. 51, no. 7, pp. 1842–1851, Jul. 2003.

[9] M. Movahhedi and A. Abdipour, "Improvement of active microwave device modeling using filter-bank transforms," in *Proc. 35th Eur. Microw. Conf.*, Paris, France, Oct. 2005, pp. 1113–1117.

[10] T. Namiki, "3-D ADI-FDTD method—Unconditionally stable time-domain algorithm for solving full vector Maxwells equations," *IEEE Trans. Microw. Theory Tech.*, vol. 48, no. 10, pp. 1743–1748, Oct. 2000.

[11] F. Zheng, Z. Chen, and J. Zhang, "Toward the development of a three-dimensional unconditionally stable finite-difference time-domain method," *IEEE Trans. Microw. Theory Tech.*, vol. 48, no. 9, pp. 1550–1558, Sep. 2000.

[12] T. Grasser, T.-W. Tang, H. Kosina, and S. Selberherr, "A review of hydrodynamic and energy-transport models for semiconductor device simulation," *Proc. IEEE*, vol. 91, no. 2, pp. 251–274, Feb. 2003.

[13] Y. K. Feng and A. Hintz, "Simulation of submicrometer GaAs MESFET's using a full dynamic transport model," *IEEE Trans. Electron Devices*, vol. 35, no. 9, pp. 1419–1431, Sep. 1988.

[14] K. Tomizawa, *Numerical Simulation of Submicron Semiconductor Devices*. Norwood, MA: Artech House, 1993.

[15] K. S. Yee, "Numerical solution of initial boundary value problems involving Maxwell's equations in isotropic media," *IEEE Trans. Antenna Propag.*, vol. AP-14, no. 8, pp. 302–307, Aug. 1966.

[16] Y. Saad, *Iterative Methods for Sparse Linear Systems*. Boston, MA: PWS, 1996.

[17] Y. A. Hussein and S. M. El-Ghazaly, "Modeling and optimization of microwave devices and circuits using genetic algorithms," *IEEE Trans. Microw. Theory Tech.*, vol. 52, no. 1, pp. 329–336, Jan. 2004.

[18] H. Deng and H. Ling, "An efficient wavelet preconditioner for iterative solution of three-dimensional electromagnetic integral equations," *IEEE Trans. Antennas Propag.*, vol. 51, no. 3, pp. 654–660, Mar. 2003.

[19] A. M. Bruaset, *A Survey of Preconditioned Iterative Methods*. New York, NY: Wiley, 1995.

[20] R. Weiss, *Parameter-Free Iterative Linear Solvers*. Berlin, Germany: Akademie Verlag GmbH, 1996.

[21] J. Walen, "Filter bank preconditioners for finite difference discretizations of PDEs," Dept. Sci. Comput., Uppsala Univ., Uppsala, Sweden, Tech. Rep. 198, Jul. 1997.

[22] M. Movahhedi and A. Abdipour, "Accelerating the transient simulation of semiconductor devices using filter-bank transforms," in *Proc. 13th Eur. Gallium Arsenide Other Compon. Semiconductors Applic. Symp.*, Paris, France, Oct. 2005, pp. 477–480.

[23] S. Yoganathan and S. K. Banerjee, "A new decoupled algorithm for nonstationary, transient simulations of GaAs MESFETs," *IEEE Trans. Electron Devices*, vol. 39, no. 7, pp. 1578–1587, Jul. 1992.

[24] M. Movahhedi and A. Abdipour, "Accelerating the transient simulation of semiconductor devices using filter-bank transforms," *Int. J. Numer. Mod.*, vol. 19, pp. 47–67, Jan.–Feb. 2006.

[25] G. Liu and S. D. Gedney, "Perfectly matched layer media for an unconditionally stable three-dimensional ADI-FDTD method," *IEEE Microw. Guided Wave Lett.*, vol. 10, no. 7, pp. 261–263, Jul. 2000.

[26] S. D. Gedney, G. Liu, J. A. Roden, and A. Zhu, "Perfectly matched layer media with CFS for an unconditionally stable ADI-FDTD method," *IEEE Trans. Antennas Propag.*, vol. 49, no. 11, pp. 1554–1559, Nov. 2001.

[27] F. Zheng and Z. Chen, "Numerical dispersion analysis of the unconditionally stable 3-D ADI-FDTD method," *IEEE Trans. Microw. Theory Tech.*, vol. 49, no. 5, pp. 1006–1009, May 2001.

[28] A. P. Zhao, "The influence of the time step on the numerical dispersion error of an unconditionally stable 3-D ADI-FDTD method: A simple and unified approach to determine the maximum allowable time step required by a desired numerical dispersion accuracy," *Microw. Opt. Technol. Lett.*, vol. 35, pp. 60–65, Oct. 2002.

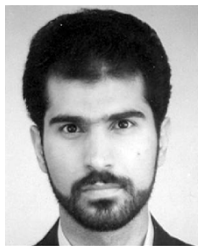

Masoud Movahhedi (S'06) was born in Yazd, Iran, in 1976. He received the B.Sc. degree from Sharif University of Technology, Tehran, Iran, in 1998, the M.Sc. degree from AmirKabir University of Technology (Tehran Polytechnic), Tehran, Iran, in 2000, both in electrical engineering, and is currently working toward the Ph.D. degree in electrical engineering at AmirKabir University of Technology.

In December 2005, he joined the Institute for Microelectronics, Vienna University of Technology, Vienna, Austria, as a Visiting Student. His research interests are in the areas of computer-aided design of microwave integrated circuits, computational electromagnetic, semiconductor high-frequency RF modeling, and interconnect simulation.

Mr. Movahhedi was the recipient of the GAAS-05 Fellowship sponsored by the GAAS Association to young graduate researchers for his paper presented at GAAS2005. He was also the recipient of the Electrical Engineering Department Outstanding Student Award in 2006.

Abdolali Abdipour (M'97) was born in Alashtar, Iran, in 1966. He received the B.Sc. degree in electrical engineering from Tehran University, Tehran, Iran, in 1989, the M.Sc. degree in electronics from Limoges University, Limoges, France, in 1992, and the Ph.D. degree in electronic engineering from Paris XI university, Paris, France, in 1996.

He is currently an Associate Professor with the Electrical Engineering Department, Amirkabir University of Technology (Tehran Polytechnic), Tehran, Iran. He authored *Noise in Electronic Communication: Modeling, Analysis and measurement* (Amirkabir Univ. Press, 2005, in Persian). His research areas include wireless communication systems (RF technology and transceivers), RF/microwave/millimeter-wave circuit and system design, electromagnetic (EM) modeling of active devices and circuits, high-frequency electronics (signal and noise), nonlinear modeling, and analysis of microwave devices and circuits. He has authored or coauthored over 80 papers in refereed journals and local and international conferences.